

H.-J. Kretzschmar¹

Department of Technical Thermodynamics,
Zittau/Goerlitz University of Applied Sciences,
P.O. Box 1455, D-02754 Zittau, Germany
e-mail: hj.kretzschmar@hs-zigr.de

J. R. Cooper

Department of Engineering,
Queen Mary University of London,
Mile End Road, London E1 4NS, UK

A. Dittmann

Department of Technical Thermodynamics,
Technical University of Dresden, Dresden
D-01062, Germany

D. G. Friend

Physical and Chemical Properties Division,
National Institute of Standards and Technology,
325 Broadway, Boulder, CO 80305

J. S. Gallagher

Physical and Chemical Properties Division,
National Institute of Standards and Technology,
100 Bureau Drive, Gaithersburg, MD 20899-8380

A. H. Harvey

Physical and Chemical Properties Division,
National Institute of Standards and Technology,
325 Broadway, MS 838.08 Boulder, CO 80305
e-mail: aharvey@boulder.nist.gov

K. Knobloch

Department of Technical Thermodynamics,
Zittau/Goerlitz University of Applied Sciences,
P.O. Box 1455, D-02754 Zittau, Germany

R. Mareš

Department of Thermodynamics,
University of West Bohemia, Univerzitní 8,
Plzeň CZ 306 14, Czech Republic

K. Miyagawa

4-12-11-628 Nishiogu,
Arakawa-ku Tokyo 116-0011, Japan

N. Okita

Thermal Plant Systems Project Department,
Toshiba Corporation, 1-1, Shibaura 1-chome
Minato-ku, Tokyo 105-8001, Japan

I. Stöcker

Department of Technical Thermodynamics,
Zittau/Goerlitz University of Applied Sciences,
P.O. Box 1455, D-02754 Zittau, Germany

W. Wagner

Lehrstuhl für Thermodynamik, Ruhr-Universität
Bochum, Bochum D-44780, Germany

I. Weber

Siemens AG, PG ER4,
Freyeslebenstr. 1,
D-91058 Erlangen,
Germany

Supplementary Backward Equations $T(p, h)$, $v(p, h)$, and $T(p, s)$, $v(p, s)$ for the Critical and Supercritical Regions (Region 3) of the Industrial Formulation IAPWS-IF97 for Water and Steam

In modeling advanced steam power cycles, thermodynamic properties as functions of pressure and enthalpy (p, h) or pressure and entropy (p, s) are required in the critical and supercritical regions (region 3 of IAPWS-IF97). With IAPWS-IF97, these calculations require cumbersome two-dimensional iteration of temperature T and specific volume v from (p, h) or (p, s). While these calculations in region 3 are not frequently required, the computing time can be significant. Therefore, the International Association for the Properties of Water and Steam (IAPWS) adopted backward equations for $T(p, h)$, $v(p, h)$, $T(p, s)$, and $v(p, s)$ in region 3, along with boundary equations for the saturation pressure as a function of enthalpy, $p_{\text{sat}}(h)$, and of entropy, $p_{\text{sat}}(s)$. Using the new equations, two-dimensional iteration can be avoided. The numerical consistency of temperature and specific volume obtained in this way is sufficient for most uses. This paper summarizes the need and the requirements for these equations and gives complete numerical information. In addition, numerical consistency and computational speed are discussed. [DOI: 10.1115/1.2181598]

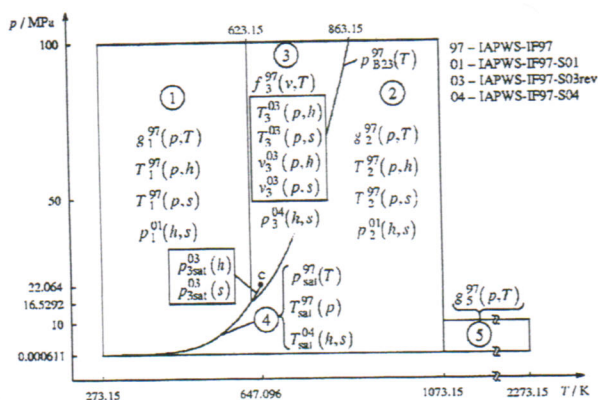


Fig. 1 Regions and equations of IAPWS-IF97, IAPWS-IF97-S01, IAPWS-IF97-S04, and the backward equations $T_3^{03}(p, h)$, $v_3^{03}(p, h)$, $T_3^{03}(p, s)$, and $v_3^{03}(p, s)$ and boundary equations $p_{3sat}^{03}(h)$ and $p_{3sat}^{03}(s)$ of this work

1 Introduction

In 1997, the International Association for the Properties of Water and Steam (IAPWS) adopted its formulation for industrial use for the thermodynamic properties of water and steam (IAPWS-IF97) [1,2]. IAPWS-IF97 contains fundamental equations and saturation equations; it also contains equations for the most often used backward functions $T(p, h)$ and $T(p, s)$ for the liquid region 1 and the vapor region 2; see Fig. 1.

In 2001, IAPWS-IF97 was supplemented by equations for the backward function $p(h, s)$ for regions 1 and 2 (see Fig. 1) [3,4]. This is referred to here as IAPWS-IF97-S01.

In modeling advanced steam power cycles, thermodynamic properties as functions of (p, h) or (p, s) are required in region 3. Performing these calculations with IAPWS-IF97 requires two-dimensional iteration using the functions $p(v, T)$, $h(v, T)$ or $p(v, T)$, $s(v, T)$ that can be explicitly derived from the region 3 fundamental equation $f(v, T)$. While these calculations in region 3 are not frequently required, the relatively large computing time can be significant. Therefore, in 2003 IAPWS adopted backward functions $T_3^{03}(p, h)$, $v_3^{03}(p, h)$ and $T_3^{03}(p, s)$, $v_3^{03}(p, s)$ (see Fig. 1). With temperature and specific volume calculated from the new backward equations, the other properties in region 3 can be calculated using the IAPWS-IF97 basic equation $f_3^{07}(v, T)$. Subsequently, equations for the saturation pressure as a function of enthalpy $p_{3sat}^{03}(h)$ and as a function of entropy $p_{3sat}^{03}(s)$ for the saturated-liquid and saturated-vapor boundaries of region 3 (see Fig. 1) were developed. Using these boundary equations, it can be determined directly whether a state point is in the single-phase or two-phase region. The boundary equations were adopted by IAPWS in 2004 and became part of the "Revised Supplementary Release on Backward Equations for the Functions $T(p, h)$, $v(p, h)$ and $T(p, s)$, $v(p, s)$ for Region 3 of the IAPWS Industrial Formulation 1997 for the Thermodynamic Properties of Water and Steam" [5], referred to here as IAPWS-IF97-S03rev. The purpose of this paper is to document IAPWS-IF97-S03rev.

Figure 1 also shows an additional supplementary release, referred to as IAPWS-IF97-S04, which was adopted in 2004 for efficient calculation of properties in region 3 as a function of the

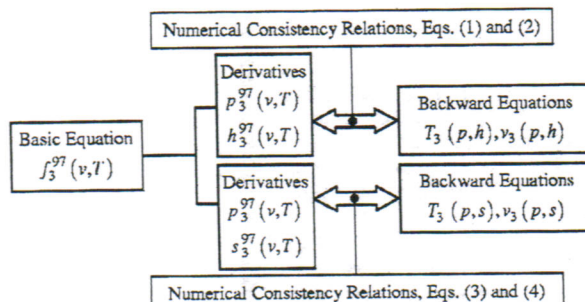


Fig. 2 Numerical consistency relations of the backward functions $T(p, h)$, $v(p, h)$, and $T(p, s)$, $v(p, s)$ with the IAPWS-IF97 basic equation $f_3^{07}(v, T)$

variables (h, s) [6]. The entire system of adopted and proposed supplementary backward equations to IAPWS-IF97 is summarized in [7].

2 Backward Equations $T(p, h)$, $v(p, h)$, $T(p, s)$, and $v(p, s)$ for Region 3

2.1 Consistency Requirements IAPWS-IF97 region 3 is covered by a basic equation for the Helmholtz free energy $f_3^{07}(v, T)$; see Fig. 2. Derived from this equation are the pressure p , specific enthalpy h , and specific entropy s as functions of specific volume v and temperature T . Equations for backward functions need to be numerically consistent with the basic equation. The consistency requirements for the backward functions $T(p, h)$, $v(p, h)$, $T(p, s)$, and $v(p, s)$ can be formulated as follows:

$$|\Delta T| = |T_3[p_3^{07}(v, T), h_3^{07}(v, T)] - T| \leq |\Delta T|_{tol} \quad (1)$$

$$\left| \frac{\Delta v}{v} \right| = \left| \frac{v_3[p_3^{07}(v, T), h_3^{07}(v, T)] - v}{v} \right| \leq \left| \frac{\Delta v}{v} \right|_{tol} \quad (2)$$

$$|\Delta T| = |T_3[p_3^{07}(v, T), s_3^{07}(v, T)] - T| \leq |\Delta T|_{tol} \quad (3)$$

$$\left| \frac{\Delta v}{v} \right| = \left| \frac{v_3[p_3^{07}(v, T), s_3^{07}(v, T)] - v}{v} \right| \leq \left| \frac{\Delta v}{v} \right|_{tol} \quad (4)$$

Equation (1) means that the difference between the temperature calculated from the backward equation $T_3(p, h)$ for given values of p and h and the temperature obtained by iteration from the IAPWS-IF97 basic equation for the same p and h must be smaller than the tolerance $|\Delta T|_{tol}$. For the specific volume, Eq. (2), the similarly defined relative difference must be smaller than the tolerance $|\Delta v/v|_{tol}$. Equations (3) and (4) give similar consistency requirements for the backward functions $T(p, s)$ and $v(p, s)$.

The tolerance for consistency of the backward functions $T(p, h)$ and $T(p, s)$ with the basic equation $f(v, T)$, $|\Delta T|_{tol} = 25$ mK, was determined by IAPWS [8,9] in an international survey. $|\Delta T|_{tol}$ and other tolerances for this work are listed in Table 1.

The tolerance Δv_{tol} for consistency of the backward functions $v(p, h)$ and $v(p, s)$ can be estimated from the total differentials

Table 1 Numerical consistency values $|\Delta T|_{tol}$ of [8,9] required for $T(p, h)$ and $T(p, s)$, values $|\Delta h|_{tol}$, $|\Delta s|_{tol}$ of [11], and resulting tolerances $|\Delta v/v|_{tol}$ required for $v(p, h)$ and $v(p, s)$

$ \Delta T _{tol}$	$ \Delta h _{tol}$	$ \Delta s _{tol}$	$ \Delta v/v _{tol}$
25 mK	80 J kg ⁻¹	0.1 J kg ⁻¹ K ⁻¹	0.01%

¹To whom correspondence should be addressed.

Submitted to ASME for publication in the JOURNAL OF ENGINEERING FOR GAS TURBINES AND POWER. Manuscript received March 17, 2005; final manuscript received January 10, 2006. Review conducted by L. Langston.

$$\Delta v_{\text{tol}} = \left(\frac{\partial v}{\partial T} \right)_h \Delta T_{\text{tol}} + \left(\frac{\partial v}{\partial h} \right)_T \Delta h_{\text{tol}} \quad (5)$$

and

$$\Delta v_{\text{tol}} = \left(\frac{\partial v}{\partial T} \right)_s \Delta T_{\text{tol}} + \left(\frac{\partial v}{\partial s} \right)_T \Delta s_{\text{tol}} \quad (6)$$

where the partial derivatives are calculated from the IAPWS-IF97 basic equation [10] and Δh_{tol} and Δs_{tol} were determined for IAPWS-IF97 from a survey of power companies and related industries [11]. In order to provide conservative uncertainties, only the mean value of the smallest of the four summands of Eqs. (5) and (6) was taken for determining Δv_{tol} . Table 1 shows the resulting tolerance $|\Delta v/v|_{\text{tol}}=0.01\%$ for both $v(p, h)$ and $v(p, s)$.

2.2 Development of Equations. A major motivation for the development of IAPWS-IF97 and its supplementary backward equations was reducing computing time. Investigations during the development of IAPWS-IF97 showed that polynomials in the form of series of additions and multiplications are effective as basic terms [12]. Therefore the following general functional form was used:

$$\frac{Z(X, Y)}{Z^*} = \sum_i n_i \left(\frac{X}{X^*} + a \right)^{I_i} \left(\frac{Y}{Y^*} + b \right)^{J_i} \quad (7)$$

The final equations were found from Eq. (7) by an approximation algorithm [13–16]. The reducing parameters Z^* , X^* , and Y^* are maximum values of the corresponding property within the range of validity of the equation. The shifting parameters a and b were determined by nonlinear optimization. The exponents I_i , J_i , and coefficients n_i were determined from the structure optimization method of Wagner [17] and Setzmann and Wagner [18], which chooses the optimal terms from a bank of terms with various values of I_i and J_i . In the optimization process, the backward equations were fitted to T - v - p - h or T - v - p - s values, with p , h , and s calculated from the IAPWS-IF97 basic equation $f_3^{97}(v, T)$, for values of v and T distributed over the range of validity. The critical point was set as a constraint. The algorithm considers the computing time needed for the equation as a part of the optimization. Details of the fitting processes are given in [13,19].

2.3 Subregions. Region 3 is defined by $623.15 \text{ K} \leq T \leq 863.15 \text{ K}$ and $p_{\text{B23}}^{97}(T) \leq p \leq 100 \text{ MPa}$ (see Fig. 1), where p_{B23}^{97} represents the B23 equation of IAPWS-IF97. Investigations showed that it was not possible to meet the numerical consistency values of Table 1 with a simple equation for each function. The problem was solved by dividing region 3 into two subregions, 3a and 3b (see Fig. 3).

The boundary between subregions 3a and 3b approximates the critical isentrope $s=s_c$. In order to decide the appropriate subregion for the functions $T_3(p, h)$ and $v_3(p, h)$, the boundary equation $h_{3ab}(p)$, Eq. (8), is used; see Fig. 3. This equation is a third-degree polynomial in reduced pressure

$$\frac{h_{3ab}(p)}{h^*} = \eta(\pi) = n_1 + n_2\pi + n_3\pi^2 + n_4\pi^3 \quad (8)$$

where $\eta=h/h^*$ and $\pi=p/p^*$ with $h^*=1 \text{ kJ kg}^{-1}$ and $p^*=1 \text{ MPa}$. The coefficients n_1 to n_4 are listed in Table 2. The function $h_{3ab}(p)$ is valid from the critical point up to 100 MPa. The temperature at 100 MPa is 762.380873481 K. Equation (8) does not exactly describe the critical isentrope. The maximum specific entropy deviation is

$$|\Delta s_{3ab}|_{\text{max}} = |s_3^{97}[T_{\text{it}}^{97}(p, h_{3ab}(p)), v_{\text{it}}^{97}(p, h_{3ab}(p))] - s_c|_{\text{max}} \\ = 0.00066 \text{ kJ kg}^{-1} \text{ K}^{-1}$$

where T_{it}^{97} and v_{it}^{97} are obtained by iteration using $p_3^{97}(v, T)$ and $s_3^{97}(v, T)$ derived from the IAPWS-IF97 basic equation for region

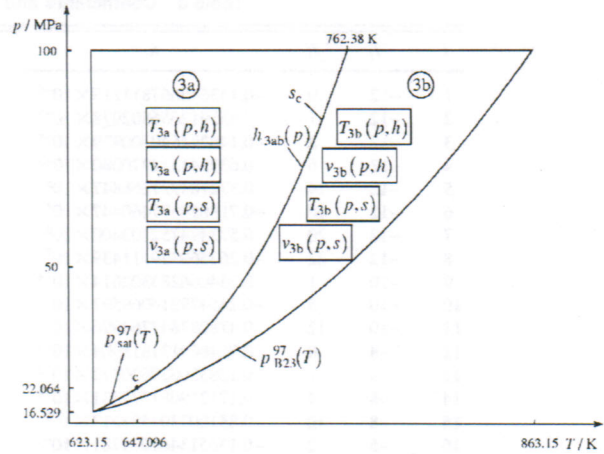


Fig. 3 Division of region 3 into subregions 3a and 3b for the backward equations $T_3(p, h)$, $v_3(p, h)$, $T_3(p, s)$, and $v_3(p, s)$

3. If the given specific enthalpy h is greater than $h_{3ab}(p)$ calculated from the given pressure p , then the state point is located in subregion 3b, otherwise it is in subregion 3a (see Fig. 3).

For the functions $T(p, s)$ and $v(p, s)$, input points can be tested directly to identify the subregion since entropy is an independent variable. If the given specific entropy s is less than or equal to

$$s_c = 4.41202148223476 \text{ kJ kg}^{-1} \text{ K}^{-1}$$

then the point is located in subregion 3a; otherwise it is in subregion 3b. The critical specific entropy s_c is given with 15 digits to avoid numerical problems.

For computer-program verification, Eq. (8) gives the following p - h point: $p=25 \text{ MPa}$, $h_{3ab}(p)=2.095936454 \times 10^3 \text{ kJ kg}^{-1}$.

2.4 Backward Equations $T(p, h)$ and $v(p, h)$

2.4.1 $T(p, h)$

2.4.1.1 Subregion 3a. The backward equation $T_{3a}(p, h)$ has the dimensionless form

$$\frac{T_{3a}(p, h)}{T^*} = \theta_{3a}(\pi, \eta) = \sum_{i=1}^{31} n_i (\pi + 0.240)^{I_i} (\eta - 0.615)^{J_i} \quad (9)$$

where $\theta=T/T^*$, $\pi=p/p^*$, and $\eta=h/h^*$ with $T^*=760 \text{ K}$, $p^*=100 \text{ MPa}$, and $h^*=2300 \text{ kJ kg}^{-1}$. The coefficients n_i and exponents I_i and J_i are listed in Table 3.

2.4.1.2 Subregion 3b. The backward equation $T_{3b}(p, h)$ is

$$\frac{T_{3b}(p, h)}{T^*} = \theta_{3b}(\pi, \eta) = \sum_{i=1}^{33} n_i (\pi + 0.298)^{I_i} (\eta - 0.720)^{J_i} \quad (10)$$

where $\theta=T/T^*$, $\pi=p/p^*$, and $\eta=h/h^*$ with $T^*=860 \text{ K}$, $p^*=100 \text{ MPa}$, and $h^*=2800 \text{ kJ kg}^{-1}$. The coefficients n_i and exponents I_i and J_i are listed in Table 4.

Table 2 Coefficients of Eq. (8)

i	n_i	i	n_i
1	0.201464004206875 $\times 10^4$	3	-0.219921901054187 $\times 10^{-1}$
2	0.374696550136983 $\times 10^1$	4	0.875131686009950 $\times 10^{-4}$

Table 3 Coefficients and exponents of Eq. (9)

i	I_i	J_i	n_i	i	I_i	J_i	n_i
1	-12	0	$-0.133645667811215 \times 10^{-6}$	17	-3	0	$-0.384460997596657 \times 10^{-5}$
2	-12	1	$0.455912656802978 \times 10^{-5}$	18	-2	1	$0.337423807911655 \times 10^{-2}$
3	-12	2	$-0.146294640700979 \times 10^{-4}$	19	-2	3	-0.551624873066791
4	-12	6	$0.639341312970080 \times 10^{-2}$	20	-2	4	0.729202277107470
5	-12	14	$0.372783927268847 \times 10^3$	21	-1	0	$-0.992522757376041 \times 10^{-2}$
6	-12	16	$-0.718654377460447 \times 10^4$	22	-1	2	-0.119308831407288
7	-12	20	$0.573494752103400 \times 10^6$	23	0	0	0.793929190615421
8	-12	22	$-0.267569329111439 \times 10^7$	24	0	1	0.454270731799386
9	-10	1	$-0.334066283302614 \times 10^{-4}$	25	1	1	0.209998591259910
10	-10	5	$-0.245479214069597 \times 10^{-1}$	26	3	0	$-0.642109823904738 \times 10^{-2}$
11	-10	12	$0.478087847764996 \times 10^2$	27	3	1	$-0.235155868604540 \times 10^{-1}$
12	-8	0	$0.764664131818904 \times 10^{-5}$	28	4	0	$0.252233108341612 \times 10^{-2}$
13	-8	2	$0.128350627676972 \times 10^{-2}$	29	4	3	$-0.764885133368119 \times 10^{-2}$
14	-8	4	$0.171219081377331 \times 10^{-1}$	30	10	4	$0.136176427574291 \times 10^{-1}$
15	-8	10	$-0.851007304583213 \times 10^1$	31	12	5	$-0.133027883575669 \times 10^{-1}$
16	-5	2	$-0.136513461629781 \times 10^{-1}$				

2.4.2 $v(p, h)$

2.4.2.1 Subregion 3a. The backward equation $v_{3a}(p, h)$ has the dimensionless form

$$\frac{v_{3a}(p, h)}{v^*} = \omega_{3a}(\pi, \eta) = \sum_{i=1}^{32} n_i (\pi + 0.128)^{I_i} (\eta - 0.727)^{J_i} \quad (11)$$

where $\omega = v/v^*$, $\pi = p/p^*$, and $\eta = h/h^*$ with $v^* = 0.0028 \text{ m}^3 \text{ kg}^{-1}$, $p^* = 100 \text{ MPa}$, and $h^* = 2100 \text{ kJ kg}^{-1}$. The coefficients n_i and exponents I_i and J_i are listed in Table 5.

2.4.2.2 Subregion 3b. The backward equation $v_{3b}(p, h)$ is

$$\frac{v_{3b}(p, h)}{v^*} = \omega_{3b}(\pi, \eta) = \sum_{i=1}^{30} n_i (\pi + 0.0661)^{I_i} (\eta - 0.720)^{J_i} \quad (12)$$

where $\omega = v/v^*$, $\pi = p/p^*$, and $\eta = h/h^*$ with $v^* = 0.0088 \text{ m}^3 \text{ kg}^{-1}$, $p^* = 100 \text{ MPa}$, and $h^* = 2800 \text{ kJ kg}^{-1}$. The coefficients n_i and exponents I_i and J_i are listed in Table 6.

2.4.3 Test Values. To assist in computer-program verification of Eqs. (9)–(12), Table 7 contains test values for calculated temperatures and specific volumes.

2.4.4 Consistency With IAPWS-IF97. The maximum and root-mean-square (RMS) differences between temperatures calculated

from Eqs. (9) and (10) and from the IAPWS-IF97 basic equation $f_3^{97}(v, T)$ are listed in Table 8. Table 8 also contains the maximum and RMS relative deviations for specific volumes from Eqs. (11) and (12) compared to IAPWS-IF97. The maximum deviations for temperature and specific volume are less than the permissible values. The critical temperature and critical volume are reproduced exactly. The RMS value is given as

$$\Delta z_{\text{RMS}} = \sqrt{\frac{1}{m} \sum_{i=1}^m (\Delta z_i)^2}$$

where Δz_i can be either the absolute or percentage difference between the corresponding quantities z and m is the number of Δz_i values (100 million points well distributed over the range of validity).

2.4.5 Consistency at the Subregion Boundary. The maximum difference between the backward equations $T_{3a}(p, h)$, Eq. (9), and $T_{3b}(p, h)$, Eq. (10), along the subregion boundary $h_{3ab}(p)$, Eq. (8), is 0.37 mK, which is smaller than the 25 mK numerical consistency specified for IAPWS-IF97. The maximum relative difference between the backward equations $v_{3a}(p, h)$, Eq. (11), and $v_{3b}(p, h)$, Eq. (12), along this boundary is 0.00015%, which is smaller than the 0.01% consistency requirement of Eqs. (11) and (12) with the IAPWS-IF97 basic equation.

Table 4 Coefficients and exponents of Eq. (10)

i	I_i	J_i	n_i	i	I_i	J_i	n_i
1	-12	0	$0.323254573644920 \times 10^{-4}$	18	-3	5	$-0.307622221350501 \times 10^1$
2	-12	1	$-0.127575556587181 \times 10^{-3}$	19	-2	0	$-0.574011959864879 \times 10^{-1}$
3	-10	0	$-0.475851877356068 \times 10^{-3}$	20	-2	4	$0.503471360939849 \times 10^1$
4	-10	1	$0.156183014181602 \times 10^{-2}$	21	-1	2	-0.925081888584834
5	-10	5	0.105724860113781	22	-1	4	$0.391733882917546 \times 10^1$
6	-10	10	$-0.858514221132534 \times 10^2$	23	-1	6	$-0.773146007130190 \times 10^2$
7	-10	12	$0.724140095480911 \times 10^3$	24	-1	10	$0.949308762098587 \times 10^4$
8	-8	0	$0.296475810273257 \times 10^{-2}$	25	-1	14	$-0.141043719679409 \times 10^7$
9	-8	1	$-0.592721983365988 \times 10^{-2}$	26	-1	16	$0.849166230819026 \times 10^7$
10	-8	2	$-0.126305422818666 \times 10^{-1}$	27	0	0	0.861095729446704
11	-8	4	-0.115716196364853	28	0	2	0.323346442811720
12	-8	10	$0.849000969739595 \times 10^2$	29	1	1	0.873281936020439
13	-6	0	$-0.108602260086615 \times 10^{-1}$	30	3	1	-0.436653048526683
14	-6	1	$0.154304475328851 \times 10^{-1}$	31	5	1	0.286596714529479
15	-6	2	$0.750455441524466 \times 10^{-1}$	32	6	1	-0.131778331276228
16	-4	0	$0.252520973612982 \times 10^{-1}$	33	8	1	$0.676682064330275 \times 10^{-2}$
17	-4	1	$-0.602507901232996 \times 10^{-1}$				

Table 5 Coefficients and exponents of Eq. (11)

i	I_i	J_i	n_i	i	I_i	J_i	n_i
1	-12	6	$0.529944062966028 \times 10^{-2}$	17	-2	16	$0.568366875815960 \times 10^4$
2	-12	8	-0.170099690234461	18	-1	0	$0.808169540124668 \times 10^{-2}$
3	-12	12	$0.111323814312927 \times 10^2$	19	-1	1	0.172416341519307
4	-12	18	$-0.217898123145125 \times 10^4$	20	-1	2	$0.104270175292927 \times 10^1$
5	-10	4	$-0.506061827980875 \times 10^{-3}$	21	-1	3	-0.297691372792847
6	-10	7	0.556495239685324	22	0	0	0.560394465163593
7	-10	10	$-0.943672726094016 \times 10^1$	23	0	1	0.275234661176914
8	-8	5	-0.297856807561527	24	1	0	-0.148347894866012
9	-8	12	$0.939353943717186 \times 10^2$	25	1	1	$-0.651142513478515 \times 10^{-1}$
10	-6	3	$0.192944939465981 \times 10^{-1}$	26	1	2	$-0.292468715386302 \times 10^1$
11	-6	4	0.421740664704763	27	2	0	$0.664876096952665 \times 10^{-1}$
12	-6	22	$-0.368914126282330 \times 10^7$	28	2	2	$0.352335014263844 \times 10^1$
13	-4	2	$-0.737566847600639 \times 10^{-2}$	29	3	0	$-0.146340792313332 \times 10^{-1}$
14	-4	3	-0.354753242424366	30	4	2	$-0.224503486668184 \times 10^1$
15	-3	7	$-0.199768169338727 \times 10^1$	31	5	2	$0.110533464706142 \times 10^1$
16	-2	3	$0.115456297059049 \times 10^1$	32	8	2	$-0.408757344495612 \times 10^{-1}$

2.5 Backward Equations $T(p, s)$ and $v(p, s)$ 2.5.1 $T(p, s)$

2.5.1.1 Subregion 3a. The backward equation $T_{3a}(p, s)$ has the dimensionless form

$$\frac{T_{3a}(p, s)}{T^*} = \theta_{3a}(\pi, \sigma) = \sum_{i=1}^{33} n_i (\pi + 0.240)^{I_i} (\sigma - 0.703)^{J_i} \quad (13)$$

where $\theta = T/T^*$, $\pi = p/p^*$, and $\sigma = s/s^*$ with $T^* = 760$ K, $p^* = 100$ MPa, and $s^* = 4.4$ kJ kg⁻¹ K⁻¹. The coefficients n_i and exponents I_i and J_i are listed in Table 9.

2.5.1.2 Subregion 3b. The backward equation $T_{3b}(p, s)$ is

$$\frac{T_{3b}(p, s)}{T^*} = \theta_{3b}(\pi, \sigma) = \sum_{i=1}^{28} n_i (\pi + 0.760)^{I_i} (\sigma - 0.818)^{J_i} \quad (14)$$

where $\theta = T/T^*$, $\pi = p/p^*$, and $\sigma = s/s^*$ with $T^* = 860$ K, $p^* = 100$ MPa, and $s^* = 5.3$ kJ kg⁻¹ K⁻¹. The coefficients n_i and exponents I_i and J_i are listed in Table 10.

2.5.2 $v(p, s)$

2.5.2.1 Subregion 3a. The backward equation $v_{3a}(p, s)$ has the dimensionless form

Table 6 Coefficients and exponents of Eq. (12)

i	I_i	J_i	n_i	i	I_i	J_i	n_i
1	-12	0	$-0.225196934336318 \times 10^{-8}$	16	-4	6	$-0.321087965668917 \times 10^1$
2	-12	1	$0.140674363313486 \times 10^{-7}$	17	-4	10	$0.607567815637771 \times 10^3$
3	-8	0	$0.233784085280560 \times 10^{-5}$	18	-3	0	$0.557686450685932 \times 10^{-3}$
4	-8	1	$-0.331833715229001 \times 10^{-4}$	19	-3	2	0.187499040029550
5	-8	3	$0.107956778514318 \times 10^{-2}$	20	-2	1	$0.905368030448107 \times 10^{-2}$
6	-8	6	-0.271382067378863	21	-2	2	0.285417173048685
7	-8	7	$0.107202262490333 \times 10^1$	22	-1	0	$0.329924030996098 \times 10^{-1}$
8	-8	8	-0.853821329075382	23	-1	1	0.239897419685483
9	-6	0	$-0.215214194340526 \times 10^{-4}$	24	-1	4	$0.482754995951394 \times 10^1$
10	-6	1	$0.769656088222730 \times 10^{-3}$	25	-1	5	$-0.118035753702231 \times 10^2$
11	-6	2	$-0.431136580433864 \times 10^{-2}$	26	0	0	0.169490044091791
12	-6	5	0.453342167309331	27	1	0	$-0.179967222507787 \times 10^{-1}$
13	-6	6	-0.507749535873652	28	1	1	$0.371810116332674 \times 10^{-1}$
14	-6	10	$-0.100475154528389 \times 10^3$	29	2	2	$-0.536288335065096 \times 10^{-1}$
15	-4	3	-0.219201924648793	30	2	6	$0.160697101092520 \times 10^1$

Table 7 Test values for temperature and specific volume calculated from Eqs. (9)–(12) for selected pressures and enthalpies

Equation	p /MPa	h /kJ kg ⁻¹	T /K	v /m ³ kg ⁻¹
$T_{3a}(p, h)$, Eq. (9)	20	1700	6.293083892×10^2	$1.749903962 \times 10^{-3}$
$v_{3a}(p, h)$, Eq. (11)	50	2000	6.905718338×10^2	$1.908139035 \times 10^{-3}$
	100	2100	7.336163014×10^2	$1.676229776 \times 10^{-3}$
$T_{3b}(p, h)$, Eq. (10)	20	2500	6.418418053×10^2	$6.670547043 \times 10^{-3}$
$v_{3b}(p, h)$, Eq. (12)	50	2400	7.351848618×10^2	$2.801244590 \times 10^{-3}$
	100	2700	8.420460876×10^2	$2.404234998 \times 10^{-3}$

Table 8 Maximum and root-mean-square differences between temperature and specific volume calculated from Eqs. (9)–(12) and those from the IAPWS-IF97 basic equation $f_3^T(v, T)$ and related tolerances

Subregion	Equation	$ \Delta T _{\text{tol}}$ (mK)	$ \Delta T _{\text{max}}$ (mK)	$ \Delta T _{\text{RMS}}$ (mK)
3a	(9)	25	23.6	10.5
3b	(10)	25	19.6	9.6
Subregion	Equation	$ \Delta v/v _{\text{tol}}$ (%)	$ \Delta v/v _{\text{max}}$ (%)	$ \Delta v/v _{\text{RMS}}$ (%)
3a	(11)	0.01	0.0080	0.0032
3b	(12)	0.01	0.0095	0.0042

$$\frac{v_{3a}(p, s)}{v^*} = \omega_{3a}(\pi, \sigma) = \sum_{i=1}^{28} n_i (\pi + 0.187)^{I_i} (\sigma - 0.755)^{J_i} \quad (15)$$

where $\omega = v/v^*$, $\pi = p/p^*$, and $\sigma = s/s^*$ with $v^* = 0.0028 \text{ m}^3 \text{ kg}^{-1}$, $p^* = 100 \text{ MPa}$, and $s^* = 4.4 \text{ kJ kg}^{-1} \text{ K}^{-1}$. The coefficients n_i and exponents I_i and J_i are listed in Table 11.

2.5.2.2 Subregion 3b. The backward equation $v_{3b}(p, s)$ is

$$\frac{v_{3b}(p, s)}{v^*} = \omega_{3b}(\pi, \sigma) = \sum_{i=1}^{31} n_i (\pi + 0.298)^{I_i} (\sigma - 0.816)^{J_i} \quad (16)$$

where $\omega = v/v^*$, $\pi = p/p^*$, and $\sigma = s/s^*$ with $v^* = 0.0088 \text{ m}^3 \text{ kg}^{-1}$, $p^* = 100 \text{ MPa}$, and $s^* = 5.3 \text{ kJ kg}^{-1} \text{ K}^{-1}$. The coefficients n_i and exponents I_i and J_i are listed in Table 12.

2.5.3 Test Values. To assist in computer-program verification of Eqs. (13)–(16), Table 13 contains test values for calculated temperatures and specific volumes.

2.5.4 Consistency with IAPWS-IF97. The maximum and RMS differences between the temperatures calculated from Eqs. (13) and (14) and the IAPWS-IF97 basic equation $f_3^T(v, T)$ in comparison with the permissible differences are listed in Table 14. Table 14 also contains the maximum and RMS relative deviations for the specific volume of Eqs. (15) and (16) from IAPWS-IF97. The maximum deviations for temperature and specific volume are less than the permissible values. The critical temperature and critical volume are reproduced exactly.

2.5.5 Consistency at the Subregion Boundary. The maximum difference between the backward equations $T_{3a}(p, s)$, Eq. (13), and $T_{3b}(p, s)$, Eq. (14), along the subregion boundary s_c is 0.093 mK. The maximum relative specific volume difference between the backward equations $v_{3a}(p, s)$, Eq. (15), and $v_{3b}(p, s)$, Eq. (16),

Table 9 Coefficients and exponents of Eq. (13)

i	I_i	J_i	n_i	i	I_i	J_i	n_i
1	-12	28	$0.150042008263875 \times 10^{10}$	18	-4	10	$-0.368275545889071 \times 10^3$
2	-12	32	$-0.159397258480424 \times 10^{12}$	19	-4	36	$0.664768904779177 \times 10^{16}$
3	-10	4	$0.502181140217975 \times 10^{-3}$	20	-2	1	$0.449359251958880 \times 10^{-1}$
4	-10	10	$-0.672057767855466 \times 10^2$	21	-2	4	$-0.422897836099655 \times 10^1$
5	-10	12	$0.145058545404456 \times 10^4$	22	-1	1	-0.240614376434179
6	-10	14	$-0.823889534888890 \times 10^4$	23	-1	6	$-0.474341365254924 \times 10^1$
7	-8	5	-0.154852214233853	24	0	0	0.724093999126110
8	-8	7	$0.112305046746695 \times 10^2$	25	0	1	0.923874349695897
9	-8	8	$-0.297000213482822 \times 10^2$	26	0	4	$0.399043655281015 \times 10^1$
10	-8	28	$0.438565132635495 \times 10^{11}$	27	1	0	$0.384066651868009 \times 10^{-1}$
11	-6	2	$0.137837838635464 \times 10^{-2}$	28	2	0	$-0.359344365571848 \times 10^{-2}$
12	-6	6	$-0.297478527157462 \times 10^1$	29	2	3	-0.735196448821653
13	-6	32	$0.971777947349413 \times 10^{13}$	30	3	2	0.188367048396131
14	-5	0	$-0.571527767052398 \times 10^{-4}$	31	8	0	$0.141064266818704 \times 10^{-3}$
15	-5	14	$0.288307949778420 \times 10^5$	32	8	1	$-0.257418501496337 \times 10^{-2}$
16	-5	32	$-0.744428289262703 \times 10^{14}$	33	10	2	$0.123220024851555 \times 10^{-2}$
17	-4	6	$0.128017324848921 \times 10^2$				

Table 10 Coefficients and exponents of Eq. (14)

i	I_i	J_i	n_i	i	I_i	J_i	n_i
1	-12	1	0.527111701601660	15	-5	6	$0.880531517490555 \times 10^3$
2	-12	3	$-0.401317830052742 \times 10^2$	16	-4	12	$0.265015592794626 \times 10^7$
3	-12	4	$0.153020073134484 \times 10^3$	17	-3	1	-0.359287150025783
4	-12	7	$-0.224799398218827 \times 10^4$	18	-3	6	$-0.656991567673753 \times 10^3$
5	-8	0	-0.193993484669048	19	-2	2	$0.241768149185367 \times 10^1$
6	-8	1	$-0.140467557893768 \times 10^1$	20	0	0	0.856873461222588
7	-8	3	$0.426799878114024 \times 10^2$	21	2	1	0.655143675313458
8	-6	0	0.752810643416743	22	3	1	-0.213535213206406
9	-6	2	$0.226657238616417 \times 10^2$	23	4	0	$0.562974957606348 \times 10^{-2}$
10	-6	4	$-0.622873556909932 \times 10^3$	24	5	24	$-0.316955725450471 \times 10^{15}$
11	-5	0	-0.660823667935396	25	6	0	$-0.699997000152457 \times 10^{-3}$
12	-5	1	0.841267087271658	26	8	3	$0.119845803210767 \times 10^{-1}$
13	-5	2	$-0.253717501764397 \times 10^2$	27	12	1	$0.193848122022095 \times 10^{-4}$
14	-5	4	$0.485708963532948 \times 10^3$	28	14	2	$-0.215095749182309 \times 10^{-4}$

Table 11 Coefficients and exponents of Eq. (15)

i	I_i	J_i	n_i	i	I_i	J_i	n_i
1	-12	10	$0.795544074093975 \times 10^2$	15	-3	2	-0.118008384666987
2	-12	12	$-0.238261242984590 \times 10^4$	16	-3	4	$0.253798642355900 \times 10^1$
3	-12	14	$0.176813100617787 \times 10^5$	17	-2	3	0.965127704669424
4	-10	4	$-0.110524727080379 \times 10^{-2}$	18	-2	8	$-0.282172420532826 \times 10^2$
5	-10	8	$-0.153213833655326 \times 10^2$	19	-1	1	0.203224612353823
6	-10	10	$0.297544599376982 \times 10^3$	20	-1	2	$0.110648186063513 \times 10^1$
7	-10	20	$-0.350315206871242 \times 10^8$	21	0	0	0.526127948451280
8	-8	5	0.277513761062119	22	0	1	0.277000018736321
9	-8	6	-0.523964271036888	23	0	3	$0.108153340501132 \times 10^1$
10	-8	14	$-0.148011182995403 \times 10^6$	24	1	0	$-0.744127885357893 \times 10^{-1}$
11	-8	16	$0.160014899374266 \times 10^7$	25	2	0	$0.164094443541384 \times 10^{-1}$
12	-6	28	$0.170802322663427 \times 10^{13}$	26	4	2	$-0.680468275301065 \times 10^{-1}$
13	-5	1	$0.246866996006494 \times 10^{-3}$	27	5	2	$0.257988576101640 \times 10^{-1}$
14	-4	5	$0.165326084797980 \times 10^1$	28	6	0	$-0.145749861944416 \times 10^{-3}$

along this boundary is 0.00046%. In both cases, the maximum difference is much smaller than numerical differences with the IAPWS-IF97 equation.

2.6 Computing Time Relative to IAPWS-IF97. A major motivation for the development of these backward equations was reducing the computing time required to obtain T and v given (p, h) or (p, s) . Using the equations developed here, the calculation is about 14 times faster than two-dimensional iteration of the IAPWS-IF97 basic equation with convergence tolerances set to the values shown in Table 1.

3 Equations $p_{\text{sat}}(h)$ and $p_{\text{sat}}(s)$ for Region 3

3.1 Determination of Region Boundaries From (p, h) and (p, s) . The boundaries between region 3 and the liquid-vapor two-phase region 4 are the saturated liquid ($x=0$) and saturated vapor ($x=1$); see Figs. 4 and 5. To identify whether a state point is located in region 4 or in region 3, iterations using the IAPWS-IF97 basic equation $f_3^{27}(v, T)$ are required to calculate the enthalpy or entropy from a given pressure on the saturation curves of region 3. The equations $p_{\text{sat}}(h)$ and $p_{\text{sat}}(s)$ provided here make it

Table 12 Coefficients and exponents of Eq. (16)

i	I_i	J_i	n_i	i	I_i	J_i	n_i
1	-12	0	$0.591599780322238 \times 10^{-4}$	17	-4	2	$-0.121613320606788 \times 10^2$
2	-12	1	$-0.185465997137856 \times 10^{-2}$	18	-4	3	$0.167637540957944 \times 10^1$
3	-12	2	$0.104190510480013 \times 10^{-1}$	19	-3	1	$-0.744135838773463 \times 10^1$
4	-12	3	$0.598647302038590 \times 10^{-2}$	20	-2	0	$0.378168091437659 \times 10^{-1}$
5	-12	5	-0.771391189901699	21	-2	1	$0.401432203027688 \times 10^1$
6	-12	6	$0.172549765557036 \times 10^1$	22	-2	2	$0.160279837479185 \times 10^2$
7	-10	0	$-0.467076079846526 \times 10^{-3}$	23	-2	3	$0.317848779347728 \times 10^1$
8	-10	1	$0.134533823384439 \times 10^{-1}$	24	-2	4	$-0.358362310304853 \times 10^1$
9	-10	2	$-0.808094336805495 \times 10^{-1}$	25	-2	12	$-0.115995260446827 \times 10^7$
10	-10	4	0.508139374365767	26	0	0	0.199256573577909
11	-8	0	$0.128584643361683 \times 10^{-2}$	27	0	1	-0.122270624794624
12	-5	1	$-0.163899353915435 \times 10^1$	28	0	2	$-0.191449143716586 \times 10^2$
13	-5	2	$0.586938199318063 \times 10^1$	29	1	0	$-0.150448002905284 \times 10^{-1}$
14	-5	3	$-0.292466667918613 \times 10^1$	30	1	2	$0.146407900162154 \times 10^2$
15	-4	0	$-0.614076301499537 \times 10^{-2}$	31	2	2	$-0.327477787188230 \times 10^1$
16	-4	1	$0.576199014049172 \times 10^1$				

Table 13 Test values for temperature and specific volume calculated from Eqs. (13)–(16) for selected pressures and entropies

Equation	p/MPa	$s/\text{kJ kg}^{-1} \text{K}^{-1}$	T/K	$v/\text{m}^3 \text{kg}^{-1}$
$T_{3a}(p, s)$, Eq. (13)	20	3.8	6.282959869×10^2	$1.733791463 \times 10^{-3}$
$v_{3a}(p, s)$, Eq. (15)	50	3.6	6.297158726×10^2	$1.469680170 \times 10^{-3}$
	100	4.0	7.056880237×10^2	$1.555893131 \times 10^{-3}$
$T_{3b}(p, s)$, Eq. (14)	20	5.0	6.401176443×10^2	$6.262101987 \times 10^{-3}$
$v_{3b}(p, s)$, Eq. (16)	50	4.5	7.163687517×10^2	$2.332634294 \times 10^{-3}$
	100	5.0	8.474332825×10^2	$2.449610757 \times 10^{-3}$

Table 14 Maximum and root-mean-square differences between the temperature and specific volume calculated from Eqs. (13)–(16) and those from the IAPWS-IF97 basic equation $g_2^T(v, T)$ and related tolerances

Subregion	Equation	$ \Delta T _{\text{tol}}$ (mK)	$ \Delta T _{\text{max}}$ (mK)	$ \Delta T _{\text{RMS}}$ (mK)
3a	(13)	25	24.8	11.2
3b	(14)	25	22.1	10.1
Subregion	Equation	$ \Delta v/v _{\text{tol}}$ (%)	$ \Delta v/v _{\text{max}}$ (%)	$ \Delta v/v _{\text{RMS}}$ (%)
3a	(15)	0.01	0.0096	0.0052
3b	(16)	0.01	0.0077	0.0037

possible to determine without iteration whether the given point is in region 4 or region 3.

The boundary between regions 1 and 3 can be calculated directly from a given pressure p and from $T=623.15$ K using the IAPWS-IF97 basic equation $g_2^T(p, T)$. The boundary between regions 2 and 3 can be calculated directly from p and from the B23 equation $T=T_{B23}^T(p)$ of IAPWS-IF97 using the basic equation $g_2^T(p, T)$.

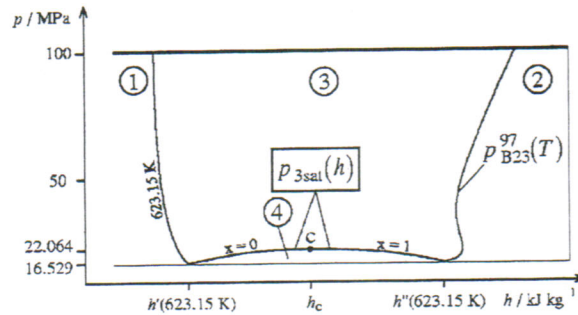


Fig. 4 IAPWS-IF97 region 3 and the boundary equation $p_{3sat}(h)$ in a p - h diagram

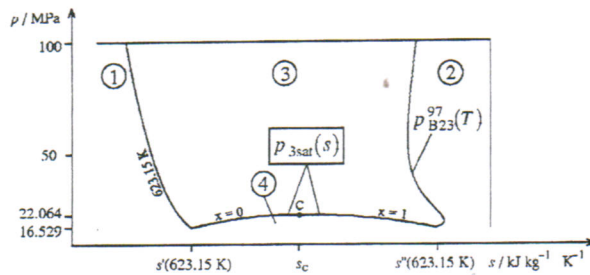


Fig. 5 IAPWS-IF97 region 3 and the boundary equation $p_{3sat}(s)$ in a p - s diagram

Table 16 Pressure values calculated from Eq. (17)

Equation	$h/\text{kJ kg}^{-1}$	p/MPa
$p_{3sat}(h)$, Eq. (17)	1700	1.724175718×10^1
	2000	2.193442957×10^1
	2400	2.018090839×10^1

3.2 Consistency Requirements. The required accuracy of the equations for the saturation boundaries of region 3 results from IAPWS requirements on backward functions. The backward functions $T(p, h)$, $v(p, h)$, $T(p, s)$, and $v(p, s)$ must fulfill their numerical consistency requirements when using $p_{3sat}(h)$ and $p_{3sat}(s)$ to determine the region for a given state point.

3.3 Boundary Equations $p_{3sat}(h)$ and $p_{3sat}(s)$

3.3.1 The Equations. $p_{3sat}(h)$ describes the saturated-liquid and saturated-vapor curves, including the critical point, in the enthalpy range (see Fig. 4):

$$h'(623.15 \text{ K}) \leq h \leq h''(623.15 \text{ K}),$$

$$\text{where } h'(623.15 \text{ K}) = 1.670858218 \times 10^3 \text{ kJ kg}^{-1}$$

$$\text{and } h''(623.15 \text{ K}) = 2.563592004 \times 10^3 \text{ kJ kg}^{-1}$$

$p_{3sat}(h)$ has the dimensionless form

$$\frac{p_{3sat}(h)}{p^*} = \pi(\eta) = \sum_{i=1}^{14} n_i (\eta - 1.02)^{I_i} (\eta - 0.608)^{J_i} \quad (17)$$

where $\pi = p/p^*$ and $\eta = h/h^*$ with $p^* = 22 \text{ MPa}$ and $h^* = 2600 \text{ kJ kg}^{-1}$. The coefficients n_i and exponents I_i and J_i are listed in Table 15.

If the given pressure p is greater than $p_{3sat}(h)$ calculated from the given enthalpy h , then the point is located in region 3, otherwise it is in region 4 (see Fig. 4). To assist in computer-program verification of Eq. (17), Table 16 contains test values for calculated pressures.

$p_{3sat}(s)$ describes the saturated-liquid and saturated-vapor curves, including the critical point, in the entropy range (see Fig. 5)

$$s'(623.15 \text{ K}) \leq s \leq s''(623.15 \text{ K}),$$

$$\text{where } s'(623.15 \text{ K}) = 3.778281340 \text{ kJ kg}^{-1} \text{ K}^{-1}$$

$$\text{and } s''(623.15 \text{ K}) = 5.210887825 \text{ kJ kg}^{-1} \text{ K}^{-1}$$

$p_{3sat}(s)$ has the dimensionless form

$$\frac{p_{3sat}(s)}{p^*} = \pi(\sigma) = \sum_{i=1}^{10} n_i (\sigma - 1.03)^{I_i} (\sigma - 0.699)^{J_i} \quad (18)$$

where $\pi = p/p^*$ and $\sigma = s/s^*$ with $p^* = 22 \text{ MPa}$ and $s^* = 5.2 \text{ kJ kg}^{-1} \text{ K}^{-1}$. The coefficients n_i and exponents I_i and J_i are

Table 15 Coefficients and exponents of Eq. (17)

i	I_i	J_i	n_i	i	I_i	J_i	n_i
1	0	0	0.600073641753024	8	8	24	$0.252304969384128 \times 10^{18}$
2	1	1	$-0.936203654849857 \times 10^1$	9	14	16	$-0.389718771997719 \times 10^{19}$
3	1	3	$0.246590798594147 \times 10^2$	10	20	16	$-0.333775713645296 \times 10^{23}$
4	1	4	$-0.107014222858224 \times 10^3$	11	22	3	$0.356499469636328 \times 10^{11}$
5	1	36	$-0.915821315805768 \times 10^{14}$	12	24	18	$-0.148547544720641 \times 10^{27}$
6	5	3	$-0.862332011700662 \times 10^4$	13	28	8	$0.330611514838798 \times 10^{19}$
7	7	0	$-0.235837344740032 \times 10^2$	14	36	24	$0.813641294467829 \times 10^{38}$

Table 17 Coefficients and exponents of Eq. (18)

i	I_i	J_i	n_i	i	I_i	J_i	n_i
1	0	0	0.639767553612785	6	12	14	$-0.378829107169011 \times 10^{18}$
2	1	1	$-0.129727445396014 \times 10^2$	7	16	36	$-0.955586736431328 \times 10^{35}$
3	1	32	$-0.224595125848403 \times 10^{16}$	8	24	10	$0.187269814676188 \times 10^{24}$
4	4	7	$0.177466741801846 \times 10^7$	9	28	0	$0.119254746466473 \times 10^{12}$
5	12	4	$0.717079349571538 \times 10^{10}$	10	32	18	$0.110649277244882 \times 10^{37}$

listed in Table 17.

If the given pressure p is greater than $p_{\text{sat}}(s)$ calculated from the given entropy s , then the point is located in region 3, otherwise it is in region 4 (see Fig. 5). To assist in computer-program verification of Eq. (18), Table 18 contains test values for calculated pressures.

3.3.2 Consistency With IAPWS-IF97 Saturation Equation. The maximum relative deviations between the calculated pressures $p_{\text{sat}}(h)$, Eq. (17), and $p_{\text{sat}}(s)$, Eq. (18), and the IAPWS-IF97 saturation equation $p_{\text{sat}}^{97}(T)$ are 0.00043% for Eq. (17) and 0.0033% for Eq. (18).

3.3.3 Consistency of Backward Equations With IAPWS-IF97 Along the Boundary Equations $p_{\text{sat}}(h)$ and $p_{\text{sat}}(s)$. The maximum temperature differences between the backward equations $T_{3a}(p, h)$, Eq. (9), and $T_{3b}(p, h)$, Eq. (10), and the IAPWS-IF97 basic equation $f_3^{97}(v, T)$ along the boundary given by $p_{\text{sat}}(h)$, Eq. (17), are shown in Table 19. Table 19 also shows the maximum percentage differences of specific volume between the backward equations $v_{3a}(p, h)$, Eq. (11), and $v_{3b}(p, h)$, Eq. (12), and the IAPWS-IF97 basic equation along $p_{\text{sat}}(h)$. The maximum differences are much smaller than the corresponding tolerances. Table 20 shows a similar comparison using the boundary equation $p_{\text{sat}}(s)$, Eq. (18). Once again, the tolerances for consistency are easily met.

3.4 Computing Time Relative to IAPWS-IF97. The motivation for the development of $p_{\text{sat}}(h)$, Eq. (17), and $p_{\text{sat}}(s)$, Eq. (18), was reducing the computing time to determine the region for a given state point (p, h) or (p, s) . With these boundary equations, this calculation is significantly faster than the iterative calculation that would otherwise be required.

Table 18 Pressure values calculated from Eq. (18)

Equation	$s/\text{kJ kg}^{-1} \text{K}^{-1}$	p/MPa
$p_{\text{sat}}(s)$, Eq. (18)	3.8	1.687755057×10^1
	4.2	2.164451789×10^1
	5.2	1.668968482×10^1

Table 19 Maximum differences of temperature and specific volume calculated by Eqs. (9)–(12) from the IAPWS-IF97 basic equation $f_3^{97}(v, T)$ along the boundary equation $p_{\text{sat}}(h)$, Eq. (17), and related tolerances

Subregion	Equation	$ \Delta T _{\text{tol}}$ (mK)	$ \Delta T _{\text{max}}$ (mK)
3a	(9)	25	0.47
3b	(10)	25	0.46
Subregion	Equation	$ \Delta v/v _{\text{tol}}$ (%)	$ \Delta v/v _{\text{max}}$ (%)
3a	(11)	0.01	0.00077
3b	(12)	0.01	0.0012

4 Application of Equations

The numerical consistency of the backward equations presented in Sec. 2 and of the boundary equations presented in Sec. 3 with the IAPWS-IF97 basic equation is sufficient for most applications in heat-cycle and boiler calculations. For users not satisfied with this consistency, these equations are recommended for generating starting points to reduce the time required for convergence of an iterative process.

These equations can only be used in the ranges of validity described in Secs. 2.3 and 3.3.1. They should not be used for determining thermodynamic derivatives. Derivatives can be determined from the IAPWS-IF97 fundamental equation $f_3^{97}(v, T)$ as described in [10]. The equations should also not be used in iterative calculations of other backward functions such as $p(h, s)$. Iteration should only be performed by using the fundamental equations of IAPWS-IF97.

In any case, depending on the application, a conscious decision is required whether to use the backward and boundary equations or to calculate the corresponding values by iteration from the basic equation of IAPWS-IF97.

5 Further Information

Further details of the numerical consistency mentioned in Secs. 2.4.4, 2.4.5, 2.5.4, 2.5.5, and 3.3.2 may be found in the dissertation of Knobloch [19]. Computer code for these equations may be obtained from the corresponding author (H.-J.K.), and links to sources for software implementing IAPWS property formulations may be found on the IAPWS website (www.iapws.org).

6 Summary

We have presented backward equations $T(p, h)$, $v(p, h)$, $T(p, s)$, and $v(p, s)$ and boundary equations $p_{\text{sat}}(h)$ and $p_{\text{sat}}(s)$ for water in IAPWS-IF97 region 3. The numerical consistencies of temperature and specific volume calculated from the backward equations with the IAPWS-IF97 basic equation $f_3^{97}(v, T)$ are sufficient for most applications in heat-cycle and boiler calculations. The new backward equations are about 14 times faster than the iterative calculation that would otherwise be needed.

The consistencies of the boundary equations $p_{\text{sat}}(h)$ and $p_{\text{sat}}(s)$ with the IAPWS-IF97 saturation equation $p_{\text{sat}}^{97}(T)$ are sufficient to

Table 20 Maximum differences of temperature and specific volume calculated by Eqs. (13)–(16) from the IAPWS-IF97 basic equation $f_3^{97}(v, T)$ along the boundary equation $p_{\text{sat}}(s)$, Eq. (18), and related tolerances

Subregion	Equation	$ \Delta T _{\text{tol}}$ (mK)	$ \Delta T _{\text{max}}$ (mK)
3a	(13)	25	2.69
3b	(14)	25	2.12
Subregion	Equation	$ \Delta v/v _{\text{tol}}$ (%)	$ \Delta v/v _{\text{max}}$ (%)
3a	(15)	0.01	0.0034
3b	(16)	0.01	0.0020

determine the region given (p, h) or (p, s) . The boundary equations are significantly faster than the iterative calculation that would otherwise be needed.

For applications where the demands on numerical consistency are extremely high, iteration using the IAPWS-IF97 equations may still be necessary. In these cases, the equations presented can be used to generate very accurate starting values.

Acknowledgment

The authors are indebted to other members of the IAPWS Working Groups "Industrial Requirements and Solutions" and "Thermophysical Properties of Water and Steam." We are grateful to all IAPWS colleagues who contributed to the project of the development of supplementary equations for IAPWS-IF97. Two of us (H.-J.K. and K.K.) are particularly grateful to the Saxony State Ministry of Science and Art for its financial support.

Nomenclature

f	= specific Helmholtz free energy
g	= specific Gibbs free energy
h	= specific enthalpy
p	= pressure
s	= specific entropy
T	= absolute temperature
v	= specific volume
Δ	= difference in any quantity
η	= reduced enthalpy, $\eta = h/h^*$
θ	= reduced temperature, $\theta = T/T^*$
π	= reduced pressure, $\pi = p/p^*$
ρ	= density
σ	= reduced entropy, $\sigma = s/s^*$
ω	= reduced volume, $\omega = v/v^*$
n	= coefficient
I, J	= exponent
i, j	= serial number

Superscripts

97	= quantity or equation of IAPWS-IF97
01	= equation of IAPWS-IF97-S01
03	= equation of IAPWS-IF97-S03rev
04	= equation of IAPWS-IF97-04
*	= reducing quantity
'	= saturated liquid state
"	= saturated vapor state

Subscripts

1	= region 1
2	= region 2
3	= region 3
3a	= subregion 3a
3b	= subregion 3b
3ab	= boundary between subregions 3a and 3b
4	= region 4
5	= region 5
B23	= boundary between regions 2 and 3
c	= critical point
it	= iterated quantity
max	= maximum value of a quantity
RMS	= root-mean-square value of a quantity
sat	= saturation state
tol	= tolerance value of a quantity

References

- [1] International Association for the Properties of Water and Steam, 1997, "Release on the IAPWS Industrial Formulation 1997 for the Thermodynamic Properties of Water and Steam," IAPWS Release, IAPWS Secretariat, available at www.iapws.org
- [2] Wagner, W., Cooper, J. R., Dittmann, A., Kijima, J., Kretschmar, H.-J., Kruse, A., Mareš, R., Oguchi, K., Sato, H., Stöcker, I., Šifner, O., Tanishita, I.,

- Trübenbach, J., and Willkommen, Th., 2000, "The IAPWS Industrial Formulation 1997 for the Thermodynamic Properties of Water and Steam," *J. Eng. Gas Turbines Power*, **122**, pp. 150–182.
- [3] International Association for the Properties of Water and Steam, 2001, "Supplementary Release on Backward Equations for Pressure as a Function of Enthalpy and Entropy $p(h, s)$ to the IAPWS Industrial Formulation 1997 for the Thermodynamic Properties of Water and Steam," IAPWS Release, IAPWS Secretariat, available at www.iapws.org
- [4] Kretschmar, H.-J., Cooper, J. R., Dittmann, A., Friend, D. G., Gallagher, J. S., Knobloch, K., Mareš, R., Miyagawa, K., Stöcker, I., Trübenbach, J., Wagner, W., and Willkommen, Th., "Supplementary Backward Equations for Pressure as a Function of Enthalpy and Entropy $p(h, s)$ to the Industrial Formulation IAPWS-IF97 for Water and Steam," *J. Eng. Gas Turbines Power*, in press.
- [5] International Association for the Properties of Water and Steam, 2004, "Revised Supplementary Release on Backward Equations for the Functions $T(p, h)$, $v(p, h)$ and $T(p, s)$, $v(p, s)$ for Region 3 of the IAPWS Industrial Formulation 1997 for the Thermodynamic Properties of Water and Steam," IAPWS Release, IAPWS Secretariat, available at www.iapws.org
- [6] International Association for the Properties of Water and Steam, 2004, "Supplementary Release on Backward Equations $p(h, s)$ for Region 3, Equations as a Function of h and s for the Region Boundaries, and an Equation $T_{sat}(h, s)$ for Region 4 of the IAPWS Industrial Formulation 1997 for the Thermodynamic Properties of Water and Steam," IAPWS Release, IAPWS Secretariat, available at www.iapws.org
- [7] Kretschmar, H.-J., and Knobloch, K., 2005, "Supplementary Backward Equations for the Industrial Formulation IAPWS-IF97 of Water and Steam for Fast Calculations of Heat Cycles, Boilers, and Steam Turbines," in M. Nakahara et al., eds., *Water, Steam and Aqueous Solutions for Electric Power: Advances in Science and Technology, Proceedings of the 14th International Conference on the Properties of Water and Steam*, Maruzen Co., Ltd., Kyoto, Japan, pp. 34–45.
- [8] Kretschmar, H.-J., 2001, "Specifications for the Supplementary Backward Equations $T(p, h)$ and $T(p, s)$ in Region 3 of IAPWS-IF97," B. Dooley, ed., *Minutes of the Meetings of the Executive Committee of the International Association for the Properties of Water and Steam*, Gaithersburg 2001, IAPWS Secretariat, Palo Alto, CA, p. 6 and Attachment 7-Item #6.
- [9] Rukes, B., 1994, "Specifications for Numerical Consistency," B. Dooley, ed., *Minutes of the Meetings of the Executive Committee of the International Association for the Properties of Water and Steam*, Orlando, 1994, IAPWS Secretariat, Palo Alto, CA, pp. 31–33.
- [10] Kretschmar, H.-J., Stöcker, I., Klinger, J., and Dittmann, A., 2000, "Calculation of Thermodynamic Derivatives for Water and Steam Using the New Industrial Formulation IAPWS-IF97," P. R. Tremaine et al., eds., *Steam, Water and Hydrothermal Systems: Physics and Chemistry Meeting the Needs of Industry, Proceedings of the 13th International Conference on the Properties of Water and Steam*, NRC Press, Ottawa, pp. 238–247.
- [11] Rukes, B., and Wagner, W., 1991, "Final Set of Specifications for the New Industrial Formulation," B. Dooley, ed., *Minutes of the Meetings of the Executive Committee of the International Association for the Properties of Water and Steam*, Tokyo 1991, IAPWS Secretariat, Palo Alto, CA, pp. 78–82.
- [12] Kruse, A., and Wagner, W., 1998, "Neue Zustandsgleichungen für industrielle Anwendungen im technisch relevanten Zustandsgebiet von Wasser (New Equations of State for Water for Industrial Use)," *Fortschr.-Ber. VDI, Reihe 6*, Nr. 393, VDI-Verlag, Düsseldorf.
- [13] Trübenbach, J., 1999, "Ein Algorithmus zur Aufstellung rechenzeitspazierter Gleichungen für thermodynamische Zustandsgrößen (An Algorithm for Developing Equations of State Optimized Regarding Their Computing Time Consumption)," *Fortschr.-Ber. VDI, Reihe 6*, Nr. 417, VDI-Verlag, Düsseldorf.
- [14] Willkommen, Th., Kretschmar, H.-J., and Dittmann, A., 1995, "An Algorithm for Setting up Numerically Consistent Forward and Backward Equations for Process Modelling," in H. J. White et al., eds., *Physical Chemistry of Aqueous Systems, Proceedings of the 12th International Conference on the Properties of Water and Steam*, Begell House, New York, pp. 194–201.
- [15] Willkommen, Th., 1995, "Ein Algorithmus zur Aufstellung numerisch konsistenter Gleichungen für die in Prozessmodellierungen benötigten thermodynamischen Umkehrfunktionen (An Algorithm for Developing Numerically Consistent Backward Equations for Use in Process Modeling)," Dissertation, Faculty of Mechanical Engineering, Technical University of Dresden, Dresden.
- [16] Kretschmar, H.-J., 1990, "Zur Aufbereitung und Darbietung thermodynamischer Stoffdaten für die Energietechnik (The Preparation and Processing of Thermophysical Properties for Power Engineering)," Habilitation, Faculty of Mechanical Engineering, Technical University of Dresden, Dresden.
- [17] Wagner, W., 1974, "Eine mathematisch statistische Methode zum Aufstellen thermodynamischer Gleichungen—gezeigt am Beispiel der Dampfdruckkurve reiner fluider Stoffe (A Mathematical Statistical Method for Developing Equations of State—Demonstration With the Vapor Pressure Curves of Pure Fluids)," *Fortschr.-Ber. VDI, Reihe 3*, Nr. 39, VDI-Verlag, Düsseldorf.
- [18] Setzmann, W., and Wagner, W., 1989, "A New Method for Optimizing the Structure of Thermodynamic Correlation Equations," *Int. J. Thermophys.*, **10**, pp. 1103–1126.
- [19] Knobloch, K., "Gleichungen für thermodynamische Umkehrfunktionen von Wasser und Wasserdampf im kritischen und überkritischen Zustandsgebiet für energietechnische Prozessberechnungen (Equations for Thermodynamic Backward Functions of Water in the Critical and Supercritical Regions for Power Cycle Calculations)," *Fortschr.-Ber. VDI, Reihe 6*, in preparation.